

Integrative Health Systems®, LLC

"ONE CELL ONE LIGHT®"

Ms. Bonnie Kellerby

© September 5, 2018

REPORT on L/N: 30325

PHASE II: EDS/SEM Microscopy and PHASE III: Raman/Micro FTIR Spectroscopy

"Advanced Materials Specimen Collection"

RE: Bonnie Kellerby

INTRODUCTION

A collection of three (3) specimens was received by Integrative Health Systems®, LLC for Photomicrographic Imaging and Evaluation Assessment Analysis for nanotechnology as a biosensor and/or nano vehicle sensor architectural designed advanced materials. The specimens were forwarded to our contract laboratory, Applied Consumer Services, Inc., Hialeah Gardens, FL for photomicrographs of the specimen(s) (front and back). This report is known as Phase I: Photomicrographic Images (Report No. 1) dated September 5, 2018

The original specimens of were collected per chain of custody and source location as stated and delivered to Integrative Health Systems®, LLC by US Mail.

The specimens of LN 30325 underwent analysis utilizing EDS/SEM and RAMAN/Micro FTIR technologies as requested by client. If any additional analysis is requested to be performed the specimens will stay in storage as directed by client or will be returned to IHS or will be destroyed per laboratory procedures. If not identified to be returned to client at original request of initiation of this project, then the specimens are the property of Integrative Health Systems® and/or Dr. Hildegard Staninger®, RIET-1.

After all analysis and/or imaging is performed a copy of the "Chain-of-Custody" form will be attached to this report located at the end of this report with the final signature Chain-of-Custody upon final completion of all analysis to be performed. The final COC will be sent to Integrative Health Systems®, LLC from the laboratory after all work is completed and specimen not left in storage at the laboratory.

The foreign body specimen or advanced material specimen, which upon Photomicrographic imaging are sensors/electrical piece parts that have been associated with parts that are utilized in a wireless sensor body network (US Patent: 2013/0194092 A1 – Unlocking a Body Area Network Assignee Qualcomm Incorporated, San Diego, CA) is part of the collaborative research and developmental global projects that are addressed in the text book: Three-Dimensional Integration of Semiconductors: Processing, Materials and Applications by Kazuo Kondo, Morihiro Kada and Kenji Takahashi, Editors. Springer, Heidelberg, Germany © 2015. This would include the use of “invisible circuits” and their designed network systems. The individual pieces are considered nano advanced materials piece parts in the design of an integrated fusion system as applied to remote sensing technologies.

The use of waveguide designs (triangles, squares and hexagons) in pulsed systems, photovoltaic devices, nanoscale cavities and plasmonics utilizing Q factors composed of glass, disk and metal (silver) and spaser are addressed in the text book: Computational Nanophotonics: Modeling and Applications by Sarhan M. Musa, Editor. CRC Press/Taylor & Francis Group, Boca Raton, FL © 2014.

The applications of ocular biosensors and optical photonic sensors are addressed in the text: Biophotonics: Biological and Medical Physics, Biomedical Engineering by Lorenzo Pavesi and Philippe M. Fauchet (Eds.). Springer-Verlag, Berlin, East Germany © 2008.

The use of sensors, semiconductors, waveguides and other electronic components as organic electronics, i.e. the field of (opto) electronic devices utilizing organic active layers that include the following areas of organic light-emitting diodes (OLEDs), organic field-effect transistors (OFETs) and organic photovoltaics (OPVs). These nanotechnologies are utilized in the synthetic pi-conjugated small molecules and polymers, whose photoluminescence and electroluminescence span a broad spectral range; the ease of fabricating organic thin films by well-established techniques such as thermal evaporation, spin coating, and inkjet printing; and the mechanical flexibility and compatibility of organics with substrates such as glass and plastic. As a result the devices are amenable to large-scale fabrication and are expected to be of low cost. The use and development of organic electronic sensors is addressed comprehensively in the text: Organic Electronics in Sensors and Biotechnology by Ruth Shinar and Joseph Shinar. McGraw-Hill/Biophotonics, New York, New York © 2009.

Additional text book materials were utilized in the evaluation and assessment of the advanced material architectural designs of the specimens, which included the following, but were not limited to:

- 1) National Nuclear Security Administration (NNSA): Physical, Chemical and Nano Sciences Center Research Briefs, 2006 Sandia National Laboratories, Albuquerque, New Mexico.
- 2) Nanoweapons: A Growing Threat to Humanity by Louis A. Del Monte, Potomac Books, an Imprint of the University of Nebraska Press. Lincoln, Nebraska © 2017

This report will specifically address the images compared to analysis data, evaluation, assessment and results for Phase I: Photomicrographic Imaging with Phase II EDS/SEM and Phase III Raman/MicroFTIR.

The results of these scientific optical analysis results are attached to this report. The final Chain of Custody form will be forwarded to the client upon receipt from the appropriate lab(s). The Phase II: EDS/SEM Spectroscopy and Phase III Raman/Micro FTIR Microscopy Analysis Report on the selected analysis specimens will be identified in the text of this document. LN: 30325 specimens will be addressed in this report per each specimen's Object number.

PHASE II: EDS/SEM SPECTROSCOPY

Energy-dispersive X-ray spectroscopy (EDS, EDX, EDXS or XEDS), sometimes called energy dispersive X-ray analysis (EDXA) or energy dispersive X-ray microanalysis (EDXMA), is an analytical technique used for the elemental analysis or chemical characterization of a sample. It relies on an interaction of some source of X-ray excitation and a sample. Its characterization capabilities are due in large part to the fundamental principle that each element has a unique atomic structure allowing a unique set of peaks on its electromagnetic emission spectrum (which is the main principle of spectroscopy).

To stimulate the emission of characteristic X-rays from a specimen, a high-energy beam of charged particles such as electrons or protons or a beam of X-rays, is focused into the sample being studied. At rest, an atom within the sample contains ground state (or unexcited) electrons in discrete energy levels or electron shells bound to the nucleus. The incident beam may excite an electron in an inner shell, ejecting it from the shell while creating an electron hole where the electron was. An electron from an outer, higher-energy shell then fills the hole, and the difference in energy between the higher-energy shell and the lower energy shell may be released in the form of an X-ray. The number and energy of the X-rays emitted from a specimen can be measured by an energy-dispersive spectrometer. As the energies of the X-rays are characteristic of the difference in energy between the two shells and of the atomic structure of the emitting element, EDS allows the elemental composition of the specimen to be measured.

NOTE: One specimen, Object 1 was selected for Phase II and Phase III analysis.

LN 30325-1 (OBJECT 1: Red/White Particle, L. Posterior Neck)

The results of the specimen are the following for LN 30325-1:

Carbon (C)	78.25 wt %	(largest wt % element)
Oxygen (O)	25.72 wt %	
Sodium (Na)	1.44 wt %	
Silica (Si)	0.20 wt %	
Phosphorous (P)	0.25 wt %	
Sulfur (S)	0.69 wt %	
Chorine (Cl)	0.67 wt %	
Potassium (K)	0.31 wt %	

Calcium (Ca) 0.19 wt %
Iron (Fe) 0.29 wt % = 100.000 wt % Total

Noting the SEM image with a scale of 150X at 200 um (microns), where you can see specific disks that appear to be at key design areas of the fibers. They are known as Fiducial Marks. On the surface you can see the layered sheeting as well as the standard appearance of the two nano claw/hook for the waveguide edging. A small fiber wire is in the lower center that branches off from the truck of the specimen.

It should be pointed out that the "A" designs are part of the mesh network for the electric energy density within the specimen, which is for 2D and 3D designed sensors/semiconductors. The Mesh Network of Statistics address specific items such as the following: number of degrees of freedom, total number of mesh points, total number of elements, triangular elements, quadrilateral, boundary elements and vertex elements. The specimen is a of a carbonyl base due to the ratio of carbon to oxygen.

These same marks are on the LN 30325 Body area at center with a figure 8. The Fiducial Marks are clear and distinct at 200 um length at 150X. Note the " X " design and other marks. The body appears to be molded or laser etched.

PHASE III: RAMAN/Micro FTIR Microscopy

The Raman/Micro FTIR chromatographs were carefully utilized in the review of the analytical data results, because of the observation of specific peak values and the bond angles associated with the materials to better identify nano analytes within the specimens.

The Phase III results will be identified per matching Object number and what was utilized in the specimen with each peak number identified with its interpretation. When one is utilizing Raman/Micro FTIR Microscopy the presence of is detected at a molecular value and not a specific quantitative value.

LN: 30325-1 (OBJECT 1: Red/White Particle, L. Posterior Neck)

Red/White Particles

In a base of animal protein (protein, RML #1357) with the following identified chromatograph peaks:

~ **3304 cm-1** = hydrogen bonded hydroxyl stretch biomedical polymers, PCL + 1710 cm-1. Polymer of phenyl acetylene and carbon monoxide of "alternating co-polymers." (See Diagram 1.1 attached to this report.)

~ **3055 cm-1** = High polymer terephthalate denatured polyethylene terephthalates.

~ **2925 cm-1** = root rot disease of *Sesamum Indium* (Sesame "ancient seed oil). Specific signal at ~2925 cm-1 is for *Macophomia phaseolina*

~ **2852 cm-1** = Basaltic glass, Si-O or Si-O-Al a bioalteratino of textures of ethnical volcanic glass, organics and silica/silicon minerals (Ti-O; Si-O and/or Si-O-Al). The

presence of frequencies $\sim 2954, 2921, 2865$ and 2852 cm^{-1} may be present as well. If $\sim 1637 \text{ cm}^{-1}$ is present the material will contain amide I's.

$\sim 1738 \text{ cm}^{-1}$ = water with frequency $\sim 1538 \text{ cm}^{-1}$ (present was $\sim 1534 \text{ cm}^{-1}$) acetic acid cyclohexyl esters as identified by P. Mani and S. Surbert, Hindastan University Padue.

$\sim 1656 \text{ cm}^{-1}$ = Tumor diagnostic for 2D Histidine (at $\sim 1656 \text{ cm}^{-1}$) and chromosomes II at $\sim 1593, 1668$ and 1656 cm^{-1} . May have $\sim 1577 \text{ cm}^{-1}$ present.

$\sim 1534 \text{ cm}^{-1}$ = Iodine double $\sim 1534 \text{ nm}$ Diode Laser made of molecular iodine with NiPC, PdPc and PtPc ($\sim 1562, 1532$ and 1534 cm^{-1}) as metal porphorins with manganese II tetraphenylporphyrin halides, Vitamin B12 and hemoerthryin. See MnX below:

Mn (Ph₄ Por)_x Ph₄Por-tetraphenylporphyrin X = Cl⁻, Br⁻ or I⁻ Iodine = $\sim 1534 \text{ cm}^{-1}$

Cl = $\sim 1500, 1562, 1573$ and/or 1581 cm^{-1}

Br = $\sim 1499, 1457, 1564, 1574$ and/or 1582 cm^{-1}

I = $\sim 1459, 1499, \mathbf{1534}, 1562, 1573$ and/or 1583 cm^{-1}

$\sim 1454 \text{ cm}^{-1}$ = may be with 7 iodine molecules. If trace amounts of $\sim 1459 \text{ cm}^{-1}$ acetone ($\sim 1731, 1435, 3019$ and 2937 cm^{-1}) as a bimetallic magnetic chain based on oxalate complexes. Note photomicrographs had chain images on its surface. The specific $\sim 1454 \text{ cm}^{-1}$ is for SAFFORON. This material may be used as a dividing ridge material as a bar or straight lined fiduciary mark.

$\sim 1397 \text{ cm}^{-1}$ = non linear optical crystal -3-methoxy-4-hydroxyl benzaldehyde aldehyde group at $\sim 1397 \text{ cm}^{-1}$.

$\sim 1237 \text{ cm}^{-1}$ = TALAPOTAKA CHURNA as 2-chloroethyl radical in solid para-hydrogen + as reported by Jay C. Amicangelo and GC Nile, 2006. May have the following frequencies present in addition to $\sim 1237 \text{ cm}^{-1}$: $\sim 1200, 1237, 1446, 1481, 3107, 3156,$ and 3179 cm^{-1} .

$\sim 1163 \text{ cm}^{-1}$ = Tumor diagnostic, $\sim 1163 \text{ cm}^{-1}$ benign tissue and $\sim 1171 \text{ cm}^{-1}$ compared to carcinoma. Liquid Crystals (LCs) at $\sim 1762, 1672, 1600, 1163$ and 900 cm^{-1} .

$\sim 1082 \text{ cm}^{-1}$ = exfoliated human cervical cells. Signal $\sim 1082 \text{ cm}^{-1}$ symmetric phosphate (PO₂) during carcinoma. ~ 1033 and $\sim 1082 \text{ cm}^{-1}$ ethylene glycol – water complexes. "Edible coatings" Note ethylene glycol is a neurotoxin and when in a water complex matrix the bioengineered material may be in the category of 3D and 4D "pop-up design."

It is important to note that the client has experienced the transmission and receiving of signals to their ears. The benefits of a cochlear implant of innovative hearing designs may use sorption of benzene as developed by the University of South Florida with poly-

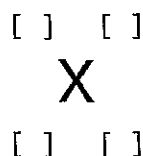
caprolactone (an FDA approved compound for drug delivery systems). A micro-patterned 3-D hydrogel bradsyn peg carbowax substances (PEG-PLA-PEG mixture) with poly (ethylene glycol) hydrogels are used in the advanced materials. The use of these materials are for Biogenic-Abiogenic interactions in natural and anthropogenic systems. US Patent 8784937 B2 (Olga V. Frank-Kamenetskaya). The use of olfenin/CO polymers are used as a new family of thermoplastics (polymeric porphyrin) ferric electro catalytic materials as used in switches as developed by PAX Consulting for US DOE.

General Comments

"as related to substances and nano building materials found in the various analysis of the specimen"

- 1) Basaltic glass – nanomicro phase ultra tiny "nano" ear can hear bacteria and viruses, LA Sudek, submarine basaltic glass colonization.
- 2) Inner Ear Images by MN Kayyali and L Brake hearing loss 134 genetic mutations, gold nano particles, liposomal iodines, and contrast dyes as Lugol's solutions or liposomal iodine.
- 3) Nanofibers called "stereocilla" for sustainable nano calcium ion channels of chopped fibers E-Glass of Basalt Si-Glass S2-glass.
- 4) 2 silicon (IV) tetraphenyl-porphyrins, Si (TPP) (py) 2 and Si (TPP) Cl₂ for 2D and 3D structures as reported by Hee-eun Song and
- 5) Molecular and crystal structure of porphyrin diacids, A. Stone, 1968.
- 6) The frequency ~ **1077 cm-1** = with ~1077 and 1083 cm-1 biofield treated metronidazole and tinidazole (CAGE) with ~1590 cm-1 cyclic acetyls of sugars. Boron is encapsulated in a complex of nano carbon material as Buckminster Fullerene, C₆₀ lithium in ammonium thin film stacked carbon as stacked Buckyballs. Used in the nano Li-ion batteries with iron and copper nano sheets and gold nanoparticles as M_xC₆₀ (M = Li, K). The nano cage is a terpenoid "cubic structure" formed by microwave irradiation from an organic resin.

These materials make fuel cells as Li⁺ C₆₀ compounds with a lithium ion beam. The design of this material has a constant shape as shown below:



The frequency ~ 1082 cm-1 was present, which is in the range of ~1083 cm-1 as stated above.

CONCLUSIONS

The correlation of the data from the EDS/SEM values and the specific peaks determined from the Raman/Micro FTIR data clearly show that the specimens taken out of the body of our client are implantable biosensory technology. The specific identification of peaks that were for three types of identifying compounds cashew nut shell, cotton cellulose, chalcogenide glasses/crystals as chrysotile, Riebeckite (asbestos nano wires) (blue color), and cotton cellulose/protein DNA nano ribbons of cotton and thiophene based materials as well as self assembling semiconductors and many other chemical derivatives clearly show that the specimens are from current nano remote sensory technology that make up an electro integrate circuit piece part system used in the monitoring of chronic diseases such as anti-coagulatives, cancer and other chronic diseases associated with pain or paralysis (Bell's palsy).

The materials identified as foreign bodies or specimens are clearly man-made nano sensor devices that are used in implantable delivery systems such as PrEPs and other formats.

The University of Arizona recently opened a Venom Institute that houses the DNA of venomous snakes as well as making a remote sensor device for monitoring HIV patients with rosasite crystals. Clinical trials of the sensors are being conducted at the Peterson Center at the University of Arizona, which is linked into other university and medical facilities for clinical trials globally. The specific venoms identified are being researched as medicines by the University of New Mexico in addition to the University of Arizona. The University of Arizona is a partner with NASA.

It is important to note that any and all of the crystals identified through the Raman analysis are microcrystals suspended in a lipidic cubic phase matrix, which as Nango, et.al stated may contradict Jardetzky's framework in how water mediates a protein (water being a liquid crystal).

It is suggested that the US Patents identified in this report be reviewed for the following:

- If they were grants.
- Universities involved in the research for the patent
- Multiple uses in a nanotechnology and remote monitoring system (telemedicine and electropharmaceuticals).
- and any other correlation.

Further correlation of the universities cited in this report to the university incubator and the assignment of technology related to the key components found in this report are necessary for the review and licensing of the technology.

It is important to note that the Peterson Center at the University of Arizona is actively involved in nano delivery system research and clinical trials with other collaborative research facilities. The university has recently developed the Venom Institute for development of venoms into medicines, such as HIV treatment, etc.

The compounds identified in the analysis clearly point to the materials being in the category of 3D Semiconductor Integrated Circuits which are composed of sensors, biosensors, nano particles, Q Factors, Q cubes and many other piece parts associated with making a smaller implantable technology through a body sensor network systems.

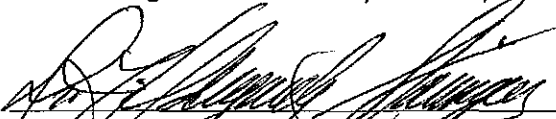
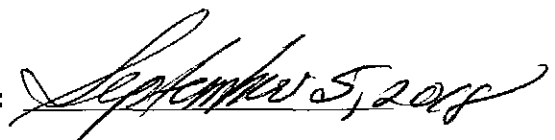
It is important to note that a type of glass (nano glass and/or Bastalic glass) was found in the analysis. These forms of glass are used with remote sensing integrated systems such as microwave, lasers, RF signals, electromagnetic systems, and many others. The glass will have organometallic complexes in it so it may also be monitored remotely through IR (Infrared) technology/cameras as well as receive a laser coupled signal or pulse wave from a nano cube satellite linked to a laser, such as Cobra Eye at MIT as well as microwave-pulsed radar transmissions.

A review of any previous reports of FCC Universal License searches and other H-SCADA methodology testing will show the primary entities involved in the signal delivery system of the implantable sensor(s) that were removed from our client. And it should be remembered that the signals will be received as long as the device (sensor/implant) is still active to receive the signal within a personal or whole body network system.

Riebkeite is used with gold nano particles and nano wires as found in venom delivery systems (lizards, ants, wasps, bee, etc.) as well as diamond rubinite as found in pirssonite that is used with biochemicals, metal complexes and peptides. These are specific materials that are used in the integration of the delivery system over a long term delivery system of approximately five or more years. A review of any early Advanced Resonance Testing would show the presence of additional small molecules as well as the affects of the sensor, chemicals and other small molecules upon our client's body as stated in a Toxicological Dysfunction Analysis Report or other format.

In summation, it is strongly suggested a complete review of previous reports be done to add to the current report and comprehensive review of the data analysis of EDS/SEM and RAMAN/Micro FTIR data as obtained from the laboratory. This will show the presence of the molecules that may not be shown in an individual specific analytical result due to the limitations of the equipment. It will show the chemical composition of the materials used and its manufacturing source or university developer/inventor through governmental and military grant funding as stated in the body of the report.

If you should need any further assistance with this report or other matters, please do not hesitate to contact Integrative Health Systems®, LLC at phone: 323-466-2599.

Signature:  **Date:** 
Dr. Heidegarde Staninger® RIEP-1
Industrial Toxicologist/IH & Doctor of Integrative Medicine
IEIA H-SCADA BioEnergy Field Professional Cert. No.: 20150911005
NREP Certified Environmental and Safety Compliance Officer
Cert. No.: 7774709608161213

Attachments:

- LN 30325 Photomicrographs and Report, dated September 5, 2018 (previously submitted as a report).
- LN 30325 Chain of Custody.
- LN 30325 EDS/SEM Spectroscopy and Raman/Micro FTIR Microscopy Results.
- Any previously submitted articles and/or documents.
- Diagram 1.1: Hydroxyl bond

REFERENCES

1. Hur, E. and DJ Moon. *Steam reforming of glycerol into hydrogen over nano-size Ni-based hydroxalcite-like catalysts*. J. Nanosci. Nanotechnology 2011 Aug; 11(8): 7394-8 (<http://www.ncbi.nlm.nih.gov/pudmed/22103204>)
2. Rivera, JA, Fetter, G and P. Bosch. *New hydroxyapatite-hydroxalcite composites II Microwave irradiation effect on structure and texture*. Journal of Porous Materials. Volume 16, Number 4, 409-418, DOI: 10, 1007/s10934-008-9213-z
3. Yin, Qing-Zhu; Cin-Ty, Aeolus Le; and Ulrich Ott. *Signatures of the s-process in presolar silicon carbide grains: Barium through Hafnium*. The Astrophysical Journal, 647:676-684, 2006 August 10
4. Dutta, Binay K., Tayseir M., Abd Ellateif, and Saikat Maitra. *Development of a porous silica film by sol-gel process*. World Academy of Science, Engineering and Technology 73 2011.
5. Dalla-Bona, Alexandra; Primbs, Jacqueline, and Angelina Angelova. *Nano-encapsulation of proteins via self-assembly with lipids and polymers*. Wiley-VCH Verlag GmbH & Co. KGaA, Weinheim, Germany © 2010 pgs 32-36
6. Dobrzhinetskaya, LF; Green, HW; Bozhilov, KN; Mitchell, TE and RM Dickerson. *Crystallization environment of Kazakhstan microdiamond: evidence from nanometric inclusion and mineral associations*. Blackwell Publishing, Ltd. 0263-4929/03. Journal of Metamorphic Geology. Volume 21, Number 21, Nov 5, 2003
7. <http://en.wikipedia.org/wiki/graphene> pgs 1 to 26 © 12/29/2011
8. Bostwirck, A. et al. *Symmetry breaking in few layer graphene films.* New Journal of Physics 9 (10) 385 © 2007
9. Zhou, S.Y., et. al. *First direct observation of Dirac fermions in graphite*. Nature Physics

2 (9): 595-599. © 2006

10. Morozov, S.V. et. al. Strong suppression of weak localization in graphene. Physical Review Letters 97 (1): 016801 © 2006
11. Kim, Kuen Soo; et al. "Large-scale pattern growth of graphene films of stretchable transparent electrodes." Nature 457 (7230) © 2009
12. Sutter, P. *Epitaxial graphene: "How silicon leaves the scene."* Nature Materials 8 (3); 171 © 2009
13. High-yield production of graphene by liquid-phase exfoliation of graphite: abstract: NatureNanotechnology(<http://www.nature.com/nnano/journal/v3/n9/abs/nano.2008.215.html>)
14. Brandenburg K. and U. Seydel. *Fourier Transform infrared spectroscopy of cell surface polysaccharides.* In: Infrared spectroscopy of biomolecules, (H.H. Mantsch and D. Chapman eds) 203-238; New York: Wiley-Liss © 1996
15. Bertoluzza A. Fagano C, Morellic MA, Gottadi, V. and MJ Guglielmi. *Raman and infrared spectra on silica gel evolving toward glass.* J. Non-Cryst. Solids, 48, 117-128 © 1982
16. Perry CC. *Biogenic silica.* In: Bio Mineralization, Chemical and Biological Perspectives. S. Mann, J. Webb and RJP Williams (eds). Chapter 8 pgs 233-256. VCH, Weinheim, Germany © 1989
17. Panick G. and R. Winter. *Pressure-Induced Unfolding/Refolding of Ribonuclease A: Static and Kinetic Fourier Transform Infrared spectroscopy Study.* Biochemistry, 39/7, 1862-1869 © 2000
18. Padmaja, P. Anikumar GM, Mukundan P, Aruldas G and KGK Warriar. *Characterizations of stoichiometric sol-gel mullite by Fourier transform infrared spectroscopy.* Int. J. of Inorg Materials 3, 693-698 © 2001
20. www.springerlink.com/index/G2266H767760104V.pdf Polyethylene-polystyrene gradient polymers II The swelling. ~730 cm⁻¹ band

www.ieeexplore.ieee.org/iel5/84/32479/01516171.pdf?arnumber=1516171 Polymer-based wide-bandwidth and high-sensitivity micro machined tunneling accelerometer, chemical sensor, infrared (IR) radiation sensor.
21. www.ieeexplore.ieee.org/iel5/3/29490/01337030.pdf?arnumber=1337030. Mid-IR Optical Limiter based on Type II Quantum Wells ~ 1493 frequency.

www.ammin.geoscienceworld.org/content/96/11-12/1856.full Methods to analyze

metastable and microparticulate hydrated related to water ~ 1463 frequency.

22. www.minsocam.org/msa/ammin/toc/.../Hammer_p569-576_98.pdf Single-crystal IR spectroscopy of very strong hydrogen bonds in pectolite at ~ 1396 cm⁻¹ frequency.
23. www.ieeeexplore.ieee.org/xpls/abs_all.jsp?arnumber=5441498 Bragg mirrors consisting of five alternating layers of Ir and porous SiO₂ are designed. ~ 1535 – 1538 frequency.
24. www.a1securitycameras.com/Samsung-Techwin-SND-3080.html

www.geo.uscb.edu/faculty/awramik/poubs/!G!SO611.pdf ~3080 cm⁻¹ bandwidths of carbonaceous material varied according to the degree of its in situ characterization.
25. Benning, Liane G.; Phoenix, VR; Yee n. and MJ Tobin. *Molecular characterization of cyanobacterial silicification using sychrontorn infrared microscopy*. Geochimica Cosmochimica Aeta. © April 16, 2003 Sychorotron-based FTIR of cyanobacteria.
26. Kneipp, Janina, et. al. *In situ identification of protein structural changes in prion-infected tissue*. Elsevier B.V. Biochimica et Biophysica Aeta 1639 (2003) 152-158
27. Gregoriou, Vasilis G. and Mark S. Braiman. *Vibrational Spectroscopy of Biological and Polymeric Materials*. CRC Press/ Taylor & Francis. Boca Raton, FL © 2006
28. <http://www.cuttingedge.org/News/n1875.cfm>
Title: DARPA is Funding an Implantable Chip Far more Advanced than "Digital Angel"
MMEA Multiple micro electrode array is far advanced it can fulfill Rev 13:16-18? Part 1 of 5 parts. © 12/29/2011
29. www.mtixtl.com Processing Routes for Aluminum based Nan-Composites. EXTEC green phenolic materials, 1100 degrees Celcius © 2010 C. Borgonova
30. Kim, Jang Sub. Samsung Electronics, Co. LED US Patent: 2007/0180954 A1 published 09-Aug-2007 . Copper nano-particles, method of preparing the same, and method of forming copper coating film using the same.
31. Stratekis, E.; Ranelia A and C. Fotakis. *Biomimetric micro/nanostructured functional surfaces for microfluidic and tissue engineering applications (3D bioimetic modification materials)*. American Institute of Physics © 30 March 2011 AIP Biomicrofluidics in Tissue Engineering and Regenerative Medicine.
32. Graham, S. et. al. *An enzyme-detergent method for effective prion decontamination of surgical steel*. Journal of General Virology. March 2005 vol. 86 no. 3 pgs 869-878
33. Kondo, Kazuo, Kada, Morhiro, Takahashi Kenji (Editors). *Three-Dimensional Integration of Semiconductors: processing, Materials and Applications*. Springer, Cham Heidelberg New York Dordredht London, Switzerland © 2015.

34. Sukhatme, Gaurav S. (Editor). The Path to Autonomous Robots. Springer, New York & Heidelberg Germany. © 2009
35. Musa, Sarhan M. (Editor). Computational Nanophotonics: Modeling and Applications. CRC Press/Taylor & Francis Group. Boca Raton, FL © 2014
36. Leszynski, Werner (Editor). Powder Metallurgy. Interscience Publishers, New York, New York © 1961.
37. Hausner, Henry H. (Editor). Modern Developments in Powder Metallurgy, Volume 2 Applications. Plenum Press, New York © 1966
38. Staninger, Hildegard. Global Brain Chip & Mesogens. Xulon Press, Inc., Maitland, FL © 2016
39. Sung, C.Y., IBM Graphene Nanoelectronics Technologies (power point presentation on IBM Website), Program Manager, IBM T.J. Watson Research Center, Science and Technology Strategy Department. POC Diagnostics and Sensing Research Capabilities and Flexible Fingerprint Sensors, July 5, 2018. www.ibm.com
40. Browne, Jack. "*MEMS Switches Shrink with Glass Substrates*." July 31, 2018
http://www.mwrf.com/comonents/mems-switches-shrink-galss-substrates?NL=MWRF-05&Issue=MWRF-05_20180801_MWRF-05_97&sfvc4enews=42&cl-article_1_b*utm_rid-CPG05000003709750&utm_campaign=18973&utm_medium=email&elqu2=778f87d03e934ada90e60e8cc4a940be

DIAGRAM 1.1: Stretching Biomedical Polymers as Alternating Co-Polymers with Specific Raman Signals.

Below is a diagram of the chemical formula showing a hydrogen bonded hydroxyl stretching of the Biomedical Polymers of PCL + 1710 cm^{-1} , polymer of phenyl acetylene and carbon monoxide as an alternating co-polymer with 3304 cm^{-1} . Carbonyl stretching occurs at 1736 cm^{-1} .

Note: PCL is known as poly-caprolactone. It degraded/metabolizes into polylactic acid (PLA). PCL may be bound to other compounds such as chitin and/or chitosan for other biomedical applications as well as thin film technologies.

Diagram of Structure

